Radiation Pattern Reconfiguration of a Patch Antenna with Metasurface for enhanced Gain and Bandwidth in 5G Millimeter-Wave Applications

Youssef EL MAIMOUNI[1,*], *Mustapha* EL HALAOUI[2], *Faouzi* RAHMANI[3], *Abdelmoumen* KAABAL[1], and *Saida* AHYOUD[1]

[1]TIMS, FS, Abdelmalek Essaadi University,Tetouan, Morocco
[2]OMS, FS, Abdelmalek Essaadi University, Tetouan, Morocco
[3]ISD, FS, Abdelmalek Essaadi University, Tetouan, Morocco

Abstract. This paper presents the design of a rectangular patch antenna intended for 5G applications. Initially, the antenna was modelled on a Rogers RT/Duroid 5880 substrate. Following optimisation of the structure's dimensions, the simulation results showed good performance at a frequency of 26 GHz. At this frequency, the antenna exhibits a reflection coefficient of -43.7 dB, a bandwidth of 0.8 GHz and a maximum gain of 8 dBi. To improve the antenna's performance, split-ring resonators (SRRs) were added to the model. Analysis of this modified structure shows an increase in bandwidth, which reaches 2 GHz. The maximum gain also increases to 12.8 dBi. PIN diodes were then incorporated into the design to control the radiation pattern. The use of these components allows the system to be reconfigured and the main lobe to be directed towards different angles. By switching the diodes between ON and OFF, the electrical properties of the metasurface are altered. This change affects the impedance and the surface current paths of the structure. Consequently, the radiated beam is redirected towards the desired directions. All stages of modelling and numerical simulation were carried out using CST Studio Suite 2022 software.

1 Introduction

Modern systems rely on fast connectivity. Antennas are the key parts in these systems. They radiate and collect electromagnetic waves. Therefore, we design and optimize these antennas to ensure clear communication.
5G technology requires high data rates, low latency and high connection capacity. To meet these requirements, reconfiguring the antenna's radiation pattern is extremely useful. This technique allows the direction and shape of the beam to be adapted to the needs of the application, which helps to resolve issues associated with the various uses of 5G.

Researchers are taking a keen interest in reconfigurable antennas [1]. The literature describes three main forms of antenna reconfiguration. These include frequency reconfiguration [2], polarization reconfiguration [3], and radiation pattern reconfiguration [4, 5]. The latter

*e-mail: youssef.elmaimouni@etu.uae.ac.ma

type modifies its radiation pattern according to the operating frequency, environmental conditions or user requirements. These antennas can alter radiation characteristics such as direction or polarization.
The main properties of antennas with reconfigurable radiation patterns are:

- **Beam Steering:** The antenna can change the direction of its main lobe to target a specific area, without the need to physically move the antenna.
- **Pattern Adjustment:** The radiation pattern can be modified to improve signal coverage and reduce interference in challenging environments.

The use of millimeter-wave (mmWave) frequencies is very important for modern telecommunications. However, these signals face challenges as they are highly sensitive to obstacles and user mobility. Reconfigurable antennas offer a practical solution for maintaining good signal coverage. Engineers use several methods to achieve this reconfiguration. These include, for example, the use of diodes [6], varactor diodes [7] and RF MEMS [8]. Metasurfaces are also utilized [5, 9], as they are well known for their ability to control the propagation of electromagnetic waves.

This work focuses on the development of a rectangular patch antenna optimized for 26 GHz operation. The aim is to reconfigure its radiation pattern to direct the main lobe towards multiple directions. To achieve this objective, we use split-ring resonators (SRRs). These elements enable precise control of wave propagation. SRRs are very useful as they modify the characteristics of the electromagnetic field. In addition to the SRRs, we incorporate PIN diodes. These diodes offer several advantages: they have low losses, are small in size, and allow for rapid state changes without the need for complex mechanical components. This structure provides the antenna with greater flexibility and improves its overall performance.

2 Antenna Design Procedure

We propose a rectangular patch antenna suitable for high-frequency 5G applications. It is based on a Rogers RT/Duroid 5880 substrate ($\epsilon_r = 2.2$, $h = 0.252$ mm). A metasurface of split-ring resonators (SRRs) is integrated into the design. By placing diodes within the SRRs, we steer the main radiation lobe to enhance both efficiency and gain.

2.1 Simple antenna without SRRs

Antenna dimensions were calculated using standard analytical formulas [7] to set the target resonant frequency. Key parameters, including dielectric constant, substrate thickness, and feed line width, were optimized to meet system specifications..

$$W_p = \frac{C}{2f_c\sqrt{\frac{\epsilon_r+1}{2}}} \tag{1}$$

$$\epsilon_{\text{eff}} = \frac{\epsilon_r + 1}{2} + \frac{\epsilon_r - 1}{2} \times \left(\frac{1}{\sqrt{1 + 12(\frac{h}{W_p})}}\right) \tag{2}$$

$$\Delta L = 0.412h \frac{(\epsilon_{\text{eff}} + 0.3)(\frac{W_p}{h} + 0.264)}{(\epsilon_{\text{eff}} - 0.258)(\frac{W_p}{h} + 0.8)} \tag{3}$$

$$L_p = \frac{C}{2f_c\sqrt{\epsilon_{\text{eff}}}} - 2\Delta L \tag{4}$$

Where W_p is the width of the patch, L_p is the length of the patch, and h is the thickness of the substrate. The symbols ϵ_r and ϵ_{eff} represent the relative permittivity and the effective permittivity of the substrate, respectively. c is the speed of light, f_c is the center frequency, and ΔL is the effective length.

Figure 1 displays the structure of the initial antenna and the model obtained after adding two slots. These slots were added to optimize the antenna behavior and tune it to the desired frequency. These modifications increase the antenna directivity.
Figure 2 presents the simulation results following these two steps. More specifically, Figure 2a shows the reflection coefficient S_{11}, where a significant improvement is observed at 26 GHz. Figure 2b shows the gain curve, which illustrates the increase in gain achieved at this same frequency. These results confirm the effectiveness of the modifications made to the structure.

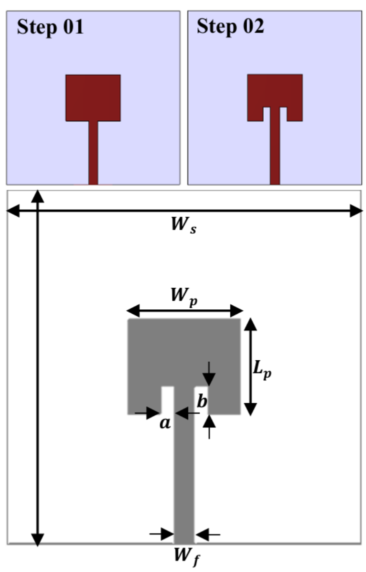

Figure 1. Geometry of patch antenna

2.2 Parametric sensitivity analysis

To ensure good performance and after calculating its dimensions using the necessary equations, it is essential to study and analyze each parameter, In this section, we analyze the impact of specific antenna dimensions on the $S11$ reflection coefficient and gain. We first evaluate the patch width sensitivity. As shown in Figure 3a, a width of 4.42 mm results in an optimal reflection coefficient of -43.7 dB at the 26 GHz frequency. In contrast, Figure 3b

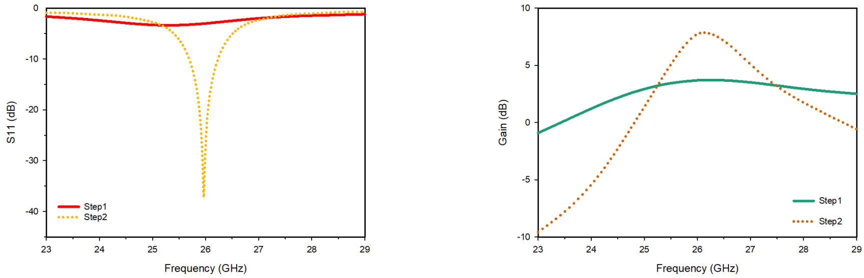

(**a**) (**b**)

Figure 2. Simulation results for the various steps: (**a**) Reflection Coefficient; (**b**) gain

Table 1. dimensions of the patch antenna

parametrs	W_p	L_p	W_f	a	b
Value (mm)	4.42	3.74	0.73	0.6	1.1

illustrates that variations in W_p values have a minor effect.
Next, the influence of patch length L_p is investigated. Figure 4a,b demonstrate how different length values impact the reflection coefficient and gain. A length of 3.74 mm is found to provide the best performance for both parameters.
Finally, Figures 5a,b and 6a,b show the effect of dimensions a and b on the reflection coefficient and the gain. For dimension a, a value of 0.6 mm yields the best performance. Similarly, for dimension b, a value of 1.1 mm provides a good balance between the reflection coefficient and the gain. These results confirm that the design parameters were chosen correctly.

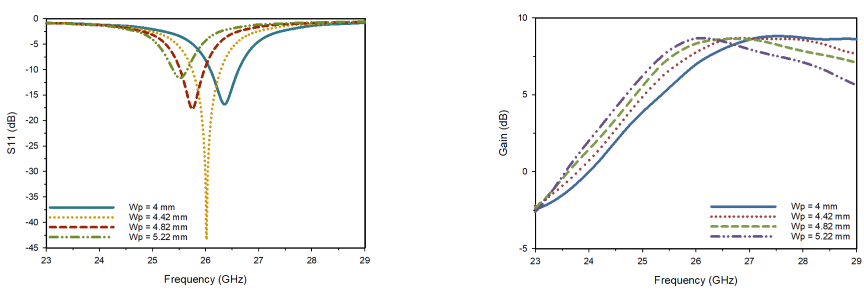

(**a**) (**b**)

Figure 3. Simulation result: influence of W_p on: (**a**) Reflection Coefficient; (**b**) gain

After analyzing the results of the study,These results were obtained following a series of simulations conducted using *CST Studio software*. the impact of specific antenna dimensions on both the reflection coefficient and gain was clearly identified. This analysis enabled the determination of the optimal values that ensure maximum antenna performance. Table 1 provides a detailed summary of these optimal dimensions, as determined through simulated and analytical results.

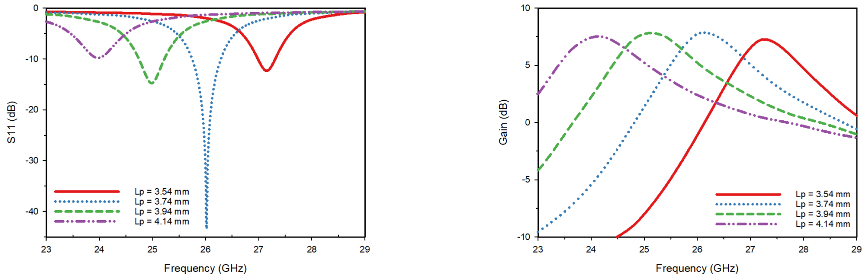

(**a**) (**b**)

Figure 4. Simulation result: influence of L_p on: (**a**) Reflection Coefficient; (**b**) gain

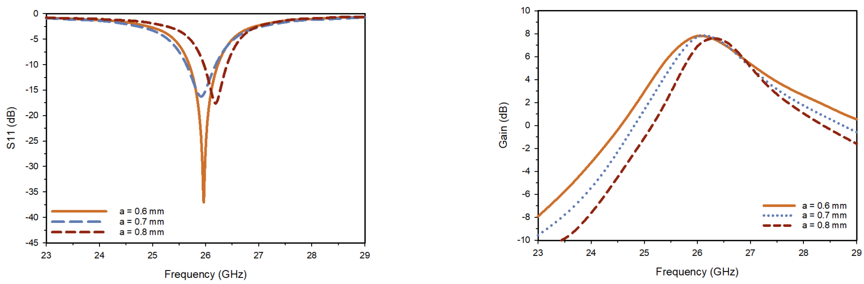

(**a**) (**b**)

Figure 5. Simulation result: influence of a on: (**a**) Reflection Coefficient; (**b**) gain

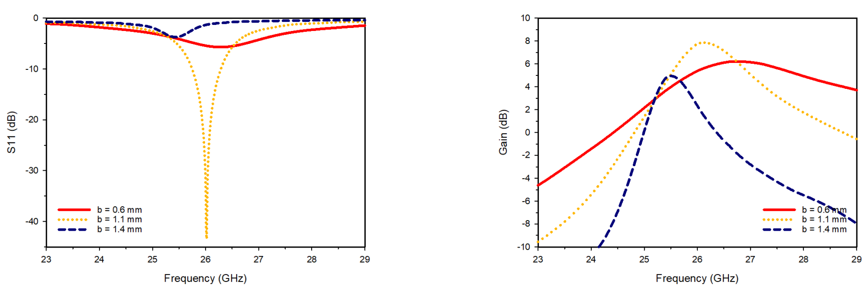

(**a**) (**b**)

Figure 6. Simulation result: influence of b on: (**a**) Reflection Coefficient; (**b**) gain

The obtained values significantly enhanced the antenna's performance. However, the primary objective of this work is to achieve a more substantial improvement in performance, while also readjusting the radiation pattern of the antenna and steering the main lobe in various directions. To this end, we propose the integration of a metasurface.

2.3 Metasurface array design

The advent of 5*G* technology has presented the field of wireless communication with a multitude of challenges, notably the effective control of electromagnetic waves. In this context, metasurfaces emerge as a promising solution due to their exceptional capabilities in manipulating electromagnetic fields. Figure 7a illustrates the design of Split-Ring Resonators that will be employed for the reconfigurable beamforming of the antenna radiation pattern. Following simulation, Figure 7b demonstrates that the unit cell resonates strongly at 26 GHz, with a reflection coefficient of −57.13 dB.

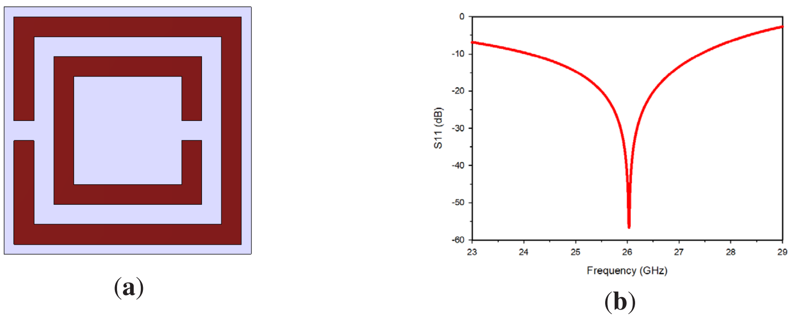

Figure 7. (**a**) Geometrie of unit cell; (**b**) Simulated Reflection Coefficient of unit cell

In order to reconfigure the antenna's radiation pattern and precisely orient the main lobe towards the target direction, a metasurface has been strategically integrated into its structure. Specifically, a matrix of Split Ring Resonator (SRRs) unit cells, arranged in a 7×2 configuration, is incorporated at the ground plane level. Additionally, two more-unit cells are positioned near the radiating element (patch), as illustrated in Figure 8.

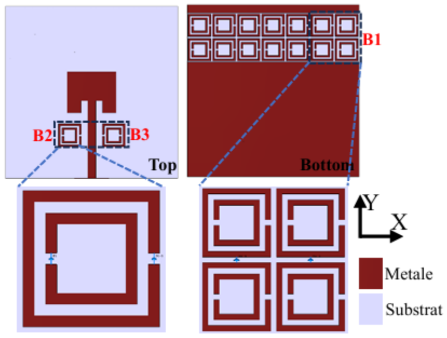

Figure 8. Geometry of proposed antenna

3 SIMULATED RESULTS AND DISCUSION

Before incorporating the metasurface, the antenna achieved a reflection coefficient of −43.7 dB at 26 GHz, with a bandwidth of 800 MHz.. After the metasurface was incorporated, a significant increase in bandwidth was observed, reaching approximately 2 *GHz*

(Figure 9).

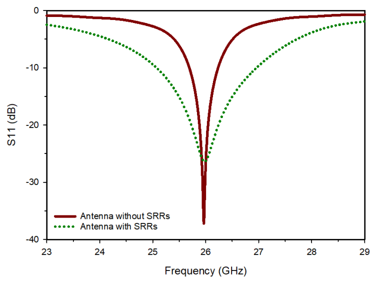

Figure 9. reflection coefficient without and with SRR

Our objective is to reconfigure the antenna's radiation pattern and steer the main lobe in various directions. To achieve this, Split Ring Resonators are utilized, as they play a fundamental role in modifying the antenna's radiation characteristics. As sub-wavelength metamaterials, SRRs exhibit unique electromagnetic properties when exposed to an incident field. Their operation relies on the excitation of localized magnetic and electric resonances. When strategically integrated into the antenna, SRRs enable local modifications of the electromagnetic boundary conditions.

To steer the main lobe in multiple directions, we integrated PIN diodes into our antenna, as shown in Figure 8. The ON or OFF state of these diodes allows us to modify the radiation pattern. The combination of PIN diodes and SRR cells is an effective method for dynamically controlling the beam. When a diode is ON, its impedance is low, and it short-circuits the metasurface. Conversely, when the diode is OFF, its impedance becomes high, allowing the SRR to function normally as designed.

The equivalent linear circuit of a PIN diode is depicted in Figure 10. In this study, the $MA4AGFCP910$ diode PIN is employed [10].In the CST model, the PIN diode is represented by equivalent RLC lumped-element circuits for both the forward- and reverse-biased states. The corresponding parameter values are listed in Table 2..

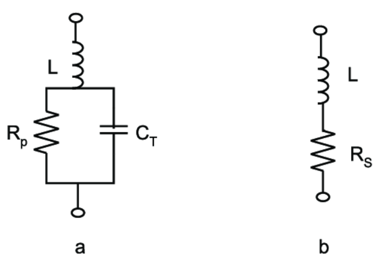

Figure 10. Equivalent circuit of PIN diode (a) reverse bias (b) forward bias

Table 2. *RLC* Equivalent Circuit Model Parameters of the PIN Diode

parametrs	C_T	R_p	R_s	L
Value	$0.018pF$	$15K\Omega$	5.2Ω	$1nH$

Table 3. Operating states of the proposed antenna

Operating states	PIN diode states			Beam direction		Gain (*dBi*)
	B1	B2	B3	XY-plan	YZ-plan	
State 1	OFF	OFF	OFF	–	0°	12.8
State 2	OFF	ON	ON	90°	41°	9.56
State 3	ON	OFF	ON	0°	17°	8.2
State 4	ON	ON	OFF	180°	−17°	8.2
State 5	ON	OFF	OFF	270°	−41°	9.56

Figure 11a illustrates the antenna's radiation pattern in the yz plane before integrating the SRRs. It is evident that the main lobe is directed towards an angle of 0°. In the xy plane (azimuth-plan), the radiation pattern exhibits omnidirectional behavior, meaning the radiation is distributed uniformly in all directions within the plane, as shown in Figure 11b.

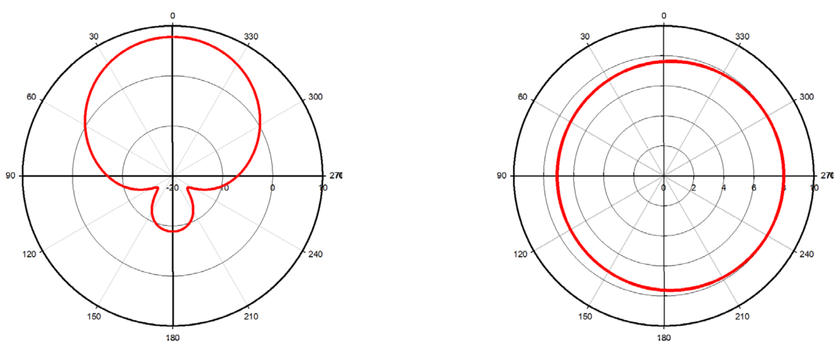

(**a**) (**b**)

Figure 11. (**a**) yz-plan radiation pattern of antenna without SRR; (**b**) xy-plan radiation pattern of antenna without SRR

To modify the antenna's radiation pattern and control the orientation of the main lobe, we adjust the state of the PIN diodes (ON or OFF). For the three block of the PIN diodes under consideration, we focus on five specific states. Table 3 summarizes the five switching states together with the corresponding main-lobe directions in the *xy* (azimuth) and *yz* (elevation) planes.

Analysis of the radiation patterns in the yz-plane (Figure 12) clearly shows that we can change the direction of our antenna's main beam. For state 1 (Figure 12a), the lobe is oriented at 0° and the maximum gain of 12.8 *dBi*, indicating very good directivity. When we switch to state 2 (Figure 12b), the lobe shifts to 41° with a gain of 9.56 *dBi*. For state 3 (Figure 12c), the lobe is positioned at 17° with a gain of 8.2 *dBi*. Symmetrically, state 4 (Figure 12d) steers the lobe at −17° (343°) with the same gain of 8.2 *dBi*. Finally, for state 5 (Figure 12e), the lobe is at −41° (319°) with a maximum gain of 9.56 *dBi*. These results confirm that our antenna can direct its beam, .with a tunable gain between 8.2 and 12.8 dBi, depending on the selected state. This flexibility in beam steering, while maintaining high gain, makes this antenna ideal for applications such as target tracking or coverage adaptation.

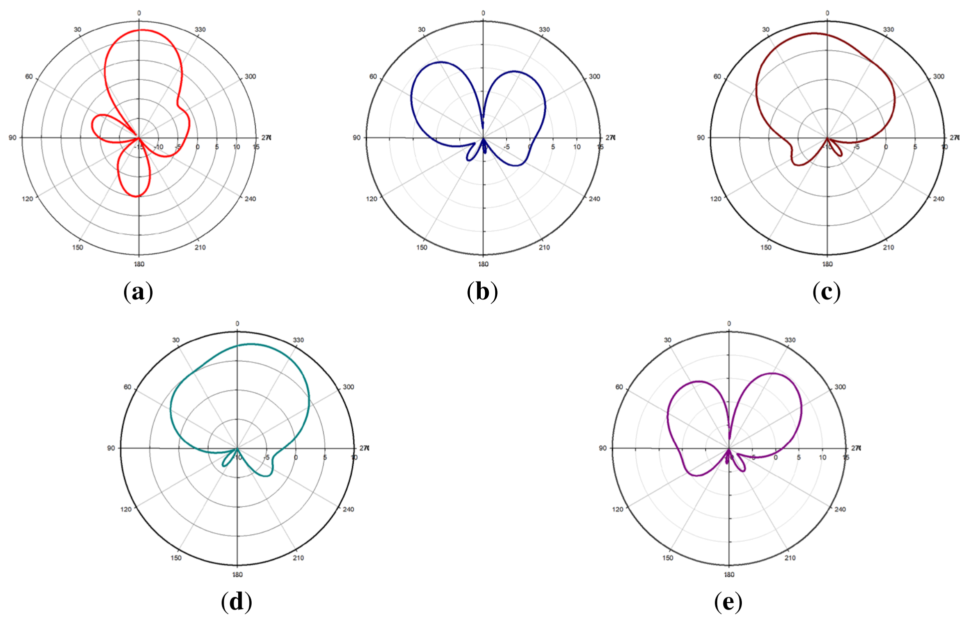

Figure 12. Simulated *yz*-plane radiation patterns: (**a**) State 1 ; (**b**) State 2 ; (**c**) State 3 ; (**d**) State 4 ; (**e**) State 5

The analysis of the radiation patterns in the *xy*-plane, presented in Figure 13 for states 2, 3, 4, and 5, demonstrates the ability of the antenna to direct the main lobe in the azimuthal plane. In state 2 (Figure 13a), the main lobe is oriented at 90°, indicating maximum directivity in that direction. When the system transitions to state 3 (Figure 13b), the main lobe is directed toward 0°. State 4 (Figure 13c) positions the main lobe at 180°, which is the opposite direction of state 3. Finally, state 5 (Figure 13d) directs the main lobe toward 270°. These observations show that the antenna can scan its main beam over 360° in the *xy*-plane, with steps of approximately 90° between successive states. This characteristic makes the antenna very useful for applications requiring sequential omnidirectional coverage or targeted azimuthal scanning.

Table 4 compares the proposed antenna with several previously published studies. The results show that our design provides strong performance, making it highly practical for wireless communication systems, particularly 5G. It reaches a high gain of 12.8 dBi, which improves signal strength and extends the coverage area. The antenna also covers a wide bandwidth of 2 GHz, showing that it can easily operate across multiple frequency bands. The main advantage of this design is its reconfigurable radiation pattern. The antenna can steer its main lobe in several different directions. This feature directs the signal more effectively toward the user and reduces interference in complex environments. By combining these features (high gain, wide bandwidth, and beam steering), this design proves to be a reliable choice for the demands of future 5G networks.

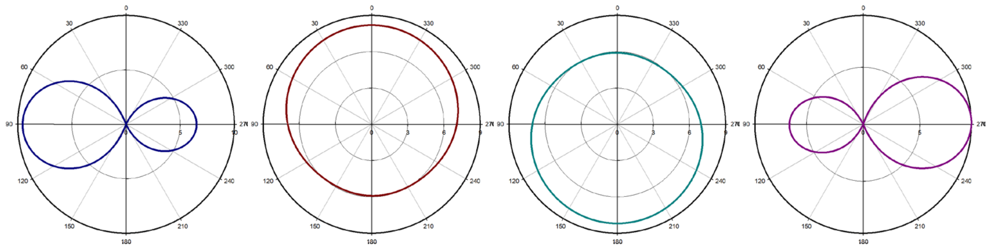

(**a**) (**b**) (**c**) (**d**)

Figure 13. Simulated *xy*-plane radiation patterns: (**a**) State 2 ; (**b**) State 3 ; (**c**) State 4 ; (**d**) State 5

Table 4. Comparison of our antenna with recent works

Ref	fr (*GHz*)	Ant. size (mm^2)	S11 (*dB*)	Reconf.	Max.Gain (*dBi*)	BW (*GHz*)
[11]	38.67	6.1×26	−47.82	NO	8.03	2.35
[12]	38	12×12	−30	NO	5.5	3
[13]	28 ; 38	7.5×8.8	−27.3	NO	5.86	1.06
[14]	28 ; 38	112×52	−39.2	YES	8.3	3.3 ; 1.2
[15]	28	12×16	−24.2	YES	5.9	-
This work	26	4.42×3.74	−43.7	YES	12.8	2

4 Conclusion

In this work, we designed a rectangular patch antenna using Rogers RT/Duroid 5880 as the substrate. We built this design step by step to fit the needs of 5G networks. We added split-ring resonators (SRRs) to improve the antenna performance and to control electromagnetic waves better. We also integrated PIN diodes into the structure. The final antenna works well at 26 GHz. It has a reflection coefficient of -43.7 dB, which shows very low losses. Finally, the design provides a wide bandwidth of 2 GHz and a maximum gain of 12.8 dBi.

The main advantage of our design is the ability to change the direction of the main beam. We can steer the main lobe in different directions by configuring the PIN diode states. The gain stays stable during these changes, with values between 8.2 dBi and 12.8 dBi. This feature, Providing high gain along with wide bandwidth, makes the antenna very useful for advanced wireless applications. Because it allows the signal to be directed as needed, it is a practical and effective solution for 5G, especially for beamforming and MIMO applications.

References

[1] T. Tandel, S. Trapasiya, Reconfigurable antenna for wireless communication: recent developments, challenges and future, Wireless Personal Communications **133**, 725 (2023). https://doi.org/10.1007/s11277-023-10785-7

[2] S. Ullah, S. Ullah, I. Ahmad, W.U.R. Khan, T. Ahmad, U. Habib, M.A. Albreem, M.H. Alsharif, P. Uthansakul, Frequency reconfigurable antenna for portable wireless applications., Computers, Materials & Continua **68** (2021). https://doi.org/10.32604/cmc.2021.015549

[3] A. Iqbal, M.I. Waly, A. Smida, N.K. Mallat, Dielectric resonator antenna with reconfigurable polarization states, IET Microwaves, Antennas & Propagation **15**, 683 (2021). https://doi.org/10.1049/mia2.12063

[4] H.P.Z. Cano, Z.D. Zaharis, T.V. Yioultsis, N.V. Kantartzis, P.I. Lazaridis, Pattern reconfigurable antennas at millimeter-wave frequencies: A comprehensive survey, IEEE Access **10**, 83029 (2022). https://doi.org/10.1109/ACCESS.2022.3196456

[5] Y. El maimouni, S. Ahyoud, A. Kaabal, Mechanical Reconfiguration of Circular Patch Antenna Using Metasurface for 5G Wireless Communications, in *International Conference on Electrical Systems & Automation* (Springer, 2023), pp. 277–283, https://doi.org/10.1007/978-3-031-51796-9_34

[6] F. Rahmani, N. Amar Touhami, A. Belbachir Kchairi, N. Aknin, N. Taher, Pattern reconfigurable antenna for vanet, wi-fi, and wimax wireless communication systems, International Journal of Antennas and Propagation **2021**, 9973839 (2021). https://doi.org/10.1155/2021/9973839

[7] C.J. You, S.H. Liu, J.X. Zhang, X. Wang, Q.Y. Li, G.Q. Yin, Z.G. Wang, Frequency- and pattern-reconfigurable antenna array with broadband tuning and wide scanning angles, IEEE Transactions on Antennas and Propagation **71**, 5398 (2023). https://doi.org/10.1109/TAP.2023.3255647

[8] P. Ssejjuuko, M. Donelli, J. Iannacci, Exploiting rf mems switches for pattern reconfigurable parasitic antennas, Micro and Nanoelectronics Devices, Circuits and Systems: Select Proceedings of MNDCS 2021 pp. 1–12 (2022). https://doi.org/10.1007/978-981-16-3767-4_1

[9] A. Chen, X. Ning, A pattern and polarization reconfigurable antenna with metasurface, International Journal of RF and Microwave Computer-Aided Engineering **31**, e22312 (2021). https://doi.org/10.1002/mmce.22312

[10] MouserElectronics, Ma4agfcp910, https://www.mouser.com/datasheet/2/249/MA4AGP907_FCP910-838114.pdf, accessed on 10 april 2025

[11] M.A. Ali, A.S. Gaid, M.M. Saeed, R.A. Saeed, Design and Performance Analysis of a 38 GHz Microstrip Patch Antenna with Slits Loading for 5G Millimeter-Wave Communications, in *2023 3rd International Conference on Emerging Smart Technologies and Applications (eSmarTA)* (IEEE, 2023), pp. 1–6, https://doi.org/10.1109/eSmarTA59349.2023.10293289

[12] A.A. Ibrahim, W.A. Ali, M. Alathbah, A.R. Sabek, Four-port 38 ghz mimo antenna with high gain and isolation for 5g wireless networks, Sensors **23**, 3557 (2023). https://doi.org/10.3390/s23073557

[13] A.E. Farahat, K.F. Hussein, Dual-band (28/38 ghz) wideband mimo antenna for 5g mobile applications, IEEe Access **10**, 32213 (2022). https://doi.org/10.1109/ACCESS.2022.3160724

[14] M.K. Shereen, M.I. Khattak, M. Al-Hasan, A frequency and radiation pattern combo-reconfigurable novel antenna for 5g applications and beyond, Electronics **9**, 1372 (2020). https://doi.org/10.3390/electronics9091372

[15] B. Ali Esmail, H.A. Majid, Z. Zainal Abidin, S. Haimi Dahlan, M. Himdi, R. Dewan, M. Kamal A Rahim, N. Al-Fadhali, Reconfigurable radiation pattern of planar antenna using metamaterial for 5g applications, Materials **13**, 582 (2020). https://doi.org/10.3390/ma13030582